J. Ocean Univ. China (Oceanic and Coastal Sea Research)
DOI 10.1007/s11802-013-2219-4
ISSN 1672-5182, 2013 12 (2): 279-286
http://www.ouc.edu.cn/xbywb/
E-mail:xbywb@ouc.edu.cn

Influence of Summer Monsoon on Asymmetric Bimodal Pattern of Tropical Cyclogenesis Frequency over the Bay of Bengal

XING Wen, and HUANG Fei*

Physical Oceanography Laboratory and Key Laboratory of Ocean-Atmosphere Interaction and Climate in Universities of Shandong, *Ocean University of China*, *Qingdao* 266100, *P. R. China*

(Received November 13, 2012; revised January 24, 2013; accepted March 5, 2013)

Abstract The influence of summer monsoon on tropical cyclone (TC) genesis over the Bay of Bengal (BoB) is explored using an empirical genesis potential (GP) index. The annual cycle of cyclogenesis frequency over the BoB shows an asymmetric bimodal pattern with the maximum genesis number appearing in late October and the second largest in early May. The two peaks correspond to the withdrawal and onset of the BoB summer monsoon, respectively. The semimonthly GP index calculated without TC days over the BoB is consistent with TC genesis frequency, indicating that the index captures the monsoon-induced changes in the environment that are responsible for the seasonal variation of TC genesis frequency. Of the four environmental variables (*i.e.*, low-level vorticity, mid-level relative humidity, potential intensity, and vertical wind shear) that enter into the GP index, the potential intensity makes the largest contribution to the bimodal distribution, followed by vertical wind shear due to small wind speed during the summer monsoon onset and withdrawal. The difference in TC genesis frequency between autumn and late spring is mainly owing to the relative humidity difference because a divergence (convergence) of horizontal moisture flux associated with cold dry northerlies (warm wet westerlies) dominates the BoB in late spring (autumn).

Key words tropical cyclone genesis; Bay of Bengal; summer monsoon; asymmetric bimodal pattern; GP index

1 Introduction

Tropical cyclones (TCs) are among the most destructive weather events that cause loss of lives and enormous property damage in affected regions. Thus, variations of TC activities have significant economic and social impact, especially in the regions with the growing afflicted population (Pielke *et al*., 2003; Emanuel, 2005). Recent work also suggested that global tropical cyclone activities may have an obvious effect on driving the ocean's thermocline circulation, which has an important influence on regional and global climate (Emanuel, 2001).

On annual average, five to six systems attain the intensity of a tropical storm with peak gusts of at least 35 knots for a sustained period of 1 min or longer in the North Indian Ocean, including both the Bay of Bengal (BoB) and the Arabian Sea (Singh *et al*., 2001). However, BoB is a region more favorable for cyclogenesis. Despite its smaller area, the number of cyclones formed in BoB is about three to four times more than that in the Arabian Sea, and the Bay generates 5% of the world's total TCs (Ali, 1996; Hoarau *et al*., 2011).

Although relatively fewer cyclones are generated in the northern Indian Ocean compared with other ocean basins across the world (Mc Bride, 1995; Lander and Guard, 1998), the cyclonegenesis in this region is characterized by a unique bimodal distribution pattern (Gray, 1968; Camargo *et al*., 2007a, b; Kikuchi and Wang, 2010; Yanase *et al*., 2010; Hoarau *et al*., 2011). It is well known that TC activities in most of ocean basins are affected by some specific modes of natural climate variability (Camargo *et al*., 2010). Similarly in the BoB, the variability in large-scale monsoon circulation also tends to have significant effects on regional TC genesis frequency. Gray (1968) conducted a global observational study of atmospheric conditions associated with tropical disturbance and storm development in each of the world's ocean basins. He identified that the North Indian Ocean tends to generate storms during the pre- and post-monsoon seasons when the monsoon trough swings across the BoB. He also noted that in the middle stage of the monsoon, TC development take place only at the very northern fringe of the BoB. The depression of cyclogenesis in July and August should be attributed to the intense vertical shear in the presence of strong easterlies in the upper troposphere (Yanase *et al*., 2012) and the seasonal dis-

* Corresponding author. Tel: 0086-532-66786326
E-mail: huangf@ouc.edu.cn

placement of the monsoon trough over the Indian subcontinent (Krishna, 2009). Subbaramayya and Rao (1984) found out that the frequency of cyclonic disturbances peaks over the BoB in the monsoon season but more than 80% of the disturbances are tropical depressions. However, the frequency of severe cyclonic storms that cause considerable damage to coastal areas reaches the maximum in the post-monsoon months.

Previous studies focused on the characteristics of TC genesis frequency mostly in the North Indian Ocean rather than the BoB. Therefore, it is not known whether the TC genesis frequency over the BoB has the same bimodal pattern as that in the North Indian Ocean. This study will focus on investigating the TC genesis mechanisms through the monsoon season, the possible linkages between the monsoon system and seasonal variations in regional cyclogenesis, and the most influential environmental factor in determining seasonal variations of TC genesis frequency over the BoB.

An empirically derived index, the Genesis Potential (GP) index, is used in this study. The GP index, developed by Emanuel and Nolan (2004), was refined from Gray's (1979) TC genesis index. The index relates tropical cyclogenesis to several important predictors and avoids using parameters that might be specific to the present climate, for instance, a specific threshold for sea surface temperature (SST) as in Gray's index, because such a SST threshold may limit the validity of Gray's index under climate change (Royer *et al*., 1998). On the other hand, the GP index can be used for different climate scenarios and in understanding the influence of large-scale circulation on tropical cyclogenesis (*e.g*., Camargo *et al*., 2007a; Camargo *et al*., 2009; Evan and Camargo, 2011). A detailed description of the GP index can be found in Camargo *et al*. (2007a).

This paper is organized as below. Section 2 describes data and methods. Section 3 presents a comparison between TC genesis frequency and GP index to evaluate the local performance of the index over the BoB region. Section 4 discusses the influence of the BoB monsoon system on the seasonal variations of the GP index by assessing the relative contribution of each predictor associated with the monsoon. Section 5 examines the differences of background conditions favorable to cyclogenesis before and after the monsoon season. Section 6 gives the conclusions.

2 Data and Methodology

The GP index, as presented by Emanuel and Nolan (2004), is defined as

$$GP = \left|10^5 \eta\right|^{3/2} \left(\frac{H}{50}\right)^3 \left(\frac{V_{\text{pot}}}{70}\right)^3 \left(1+0.1V_{\text{shear}}\right)^{-2}, \qquad (1)$$

where η is the absolute vorticity (in s^{-1}) at 850 hPa, H is the relative humidity at 700 hPa (in percent), V_{pot} is the potential intensity (in $m\,s^{-1}$), and V_{shear} is the magnitude of the vertical wind shear between 850 hPa and 200 hPa (in $m\,s^{-1}$). The potential intensity can be obtained from SST, sea level pressure, and vertical profiles of atmospheric temperature and humidity using a technique described by Emanuel (1995). More detailed information of potential intensity can be found in Bister and Emanuel (1998, 2002a, b) and Camargo *et al.* (2007a, b).

The reanalysis datasets from the National Centers for Environmental Prediction-National Center for Atmospheric Research (NCEP-NCAR) Global Reanalysis 1 for the period 1979–2008 and the SST data from the National Oceanic and Atmospheric Administration Optimum Interpolation Sea Surface Temperature V2 (NOAA OISST V2) for 1981–2008 are employed to calculate daily GP index fields. The GP data has a horizontal resolution of 2.5°. The BoB TCs in the Joint Typhoon Warning Center (JTWC) best-track dataset during the period of 1979–2008 are analyzed. The dataset contains six-hourly TC positions and intensity (http://metocph.nmci.navy.mil/jtwc/best_tracks/). JTWC best-track data for the BoB are likely to be of good quality after 1978, because the annual TC records in the datasets are consistent with the number of the observed tropical cyclones formed in the basin (Chu *et al*., 2002). Locations and times of TC genesis are defined as the first reported position and time once a TC attains the strength of a tropical depression with the maximum 1-minite sustained surface wind of greater than 34 knots.

3 Climatology of TC Genesis Frequency and GP Index over the BoB

3.1 Climatology of TC Genesis Frequency

A BoB cyclone is defined as a storm whose best-track genesis occurs in a region between 80°E and 100°E, and 2.5°N and 22.5°N. As shown in Fig.1, the blue bar represents the semimonthly number of TC genesis events over the BoB region (80°E–100°E and 2.5°N–22.5°N) from 1979 to 2008. Semimonthly datasets are used here because the genesis frequency shows significant difference between the first half and the second half months such as April and December. A total of 103 TCs occurred during the last 30 years. The TC genesis over the BoB shows a semi-annual cycle with the peak occurrences in early May and late October. Although the BoB TC is characterized by a consistent bimodal distribution as in the North Indian Ocean (Gray, 1968; Camargo *et al*., 2007; Hoarau *et al*., 2011), 41 TC events occur during early October to early November, which makes the second peak occurrence have twice as many TCs as the first one (late April to late May, total number: 20). It is also noted that the TC genesis over the Arabian Sea has no such characteristics (Evan and Camargo, 2011). Therefore, the seasonal variability of the TC genesis frequency over the BoB demonstrates a unique asymmetric bimodal pattern.

Gray (1968, 1975, 1979) revealed that tropical cyclogenesis is closely linked with regional large-scale conditions. The BoB is one of the regions under the signifi-

cant influence of the Asian-Pacific summer monsoon system (Lin and Wang, 2002). Previous studies pointed out that the onset of the BoB summer monsoon starts around early May (*e.g.*, Wu and Zhang, 1998; Wang and Lin, 2002; Mao and Wu, 2006) and withdraws in late October (Ahmed and Karmakar, 1993). Since the two genesis peak periods correspond to the onset and withdrawal of the BoB summer monsoon, it is reasonable to assume that monsoon system may have important influence on the TC genesis. In addition, the onset and withdrawal processes of the BoB summer monsoon are quasi-antisymmetric. Further investigation is still needed to understand what causes the larger number of TC events during the second peak occurrence.

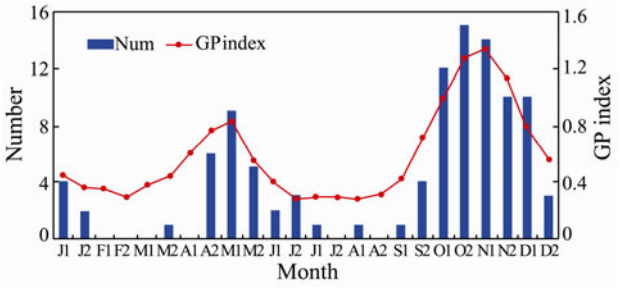

Fig.1 Seasonal cycle of the semimonthly number of TCs genesis over the BoB (blue bar) and area-averaged climatological GP index (red line) during 1979–2008.

3.2 Climatology of GP Index

Fig.2 shows the monthly climatological means of the GP index in the Indian Ocean during 1979–2008. The spatial distribution of the GP index is generally in good correspondence with TC activities in the Indian Ocean. More specifically, the seasonal variability of the GP index over the BoB agrees well with the TC genesis frequency with a weak peak in late spring and a strong one in autumn. For the Arabian Sea, the GP indexes are much smaller than those in the BoB, especially in June and October–November. The difference of the GP indexes between the Arabian Sea and BoB is consistent with that of TC genesis numbers as pointed out by Hoarau *et al.* (2011). Evan and Camargo (2011) analyzed the climatology of cyclonic storms in the Arabian Sea and found that most of the Arabian Sea cyclones form in areas close to the western coast of the Indian subcontinent, which well correspond to the areas with the peak GP index in the Arabian Sea. In the south Indian Ocean, both the GP index and the number of TC events peak in the December–February season. According to the analysis on the three individual basins, TC genesis is likely to occur in the regions with high climatological values of GP index, but not in the low GP index regions in the mentioned Indian Ocean.

It is argued that the correlation between the GP index and TC activities could be attributed to the influence of TCs on some specific factors during their life cycle. For instance, the values of vorticity and relative humidity in the middle troposphere may continue to increase throughout the lifetime of a TC and subsequently lead to a larger GP index. Based on such consideration, by disregarding

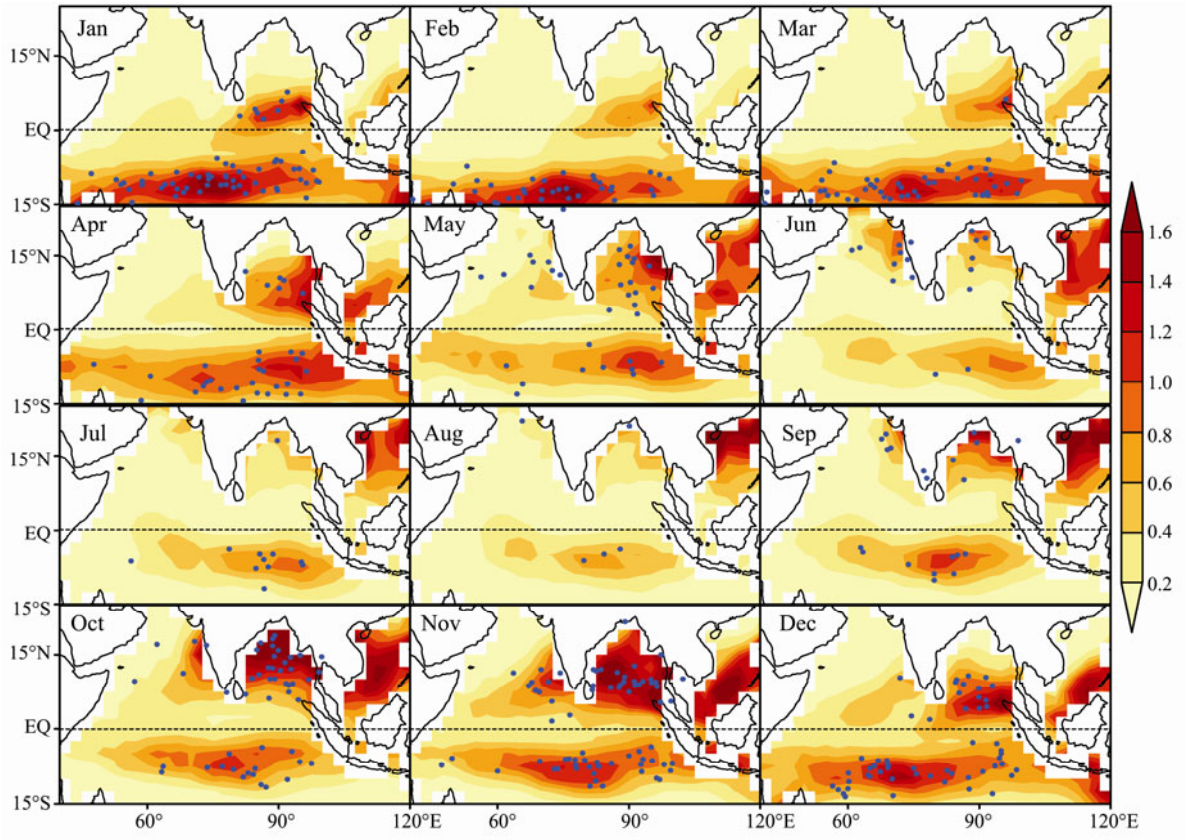

Fig.2 Monthly-mean GP index (color) and TC genesis locations (dot) over the Indian Ocean during 1979–2008.

the days when a TC exists over the BoB, semimonthly GP index values are calculated from the rest days only.

The GP index values averaged over the BoB region (80°E–100°E and 2.5°N–22.5°N) are compared in Fig.1 with the number of TCs. It can be seen that the seasonal variation of the averaged GP index corresponds to the TC numbers over the BoB, and still shows an asymmetric bimodal pattern even though the TC days are not considered in the calculations. The correlation coefficient between the number of genesis events and the semimonthly averaged GP index over the BoB is 0.934, which is statistically significant at a 99% confidence level. This good correlation demonstrates that the GP index is a good indicator of the seasonal variation of tropical cyclogenesis over the BoB. The background conditions are mostly favorable for the TC genesis in autumn and secondly in spring, which are associated with the withdrawal and onset of the monsoon system, respectively.

4 Monsoon Effects on the Semi-Annual Cycle of the TC Events

In this section, the four variables that are comprised in the GP index are assessed for the monsoon influence on TC activities. However, due to the nonlinear relationships between the GP index and those variables, it is difficult to directly separate the relative contribution of each variable. So Eq. (1) was rewritten into a logarithmic linear form as shown in Eq. (2)

$$\lg(GP)=\frac{3}{2}\lg(\left|10^5\eta\right|)+3\lg(\frac{H}{50})+3\lg(\frac{V_{\text{pot}}}{70})+\left[-2\lg(1+0.1V_{\text{shear}})\right]. \quad (2)$$

For simplification, the four components ($\frac{3}{2}\lg(\left|10^5\eta\right|)$, $3\lg(\frac{H}{50})$, $3\lg(\frac{V_{\text{pot}}}{70})$, and $[-2\lg(1+0.1V_{\text{shear}})]$) in Eq. (2) will be represented by A, B, C, D, respectively, in the following analysis. The logarithmic function of a variable is generally proportional to the variable itself. Take the GP index as an example, the correlation coefficient between the semimonthly averaged lg(*GP*), the GP index and TC number over the BoB is 0.949 and 0.871 respectively, both being statistically significant at a 99% confidence level. Thus, the seasonal cycle of lg(*GP*) can reflect the variation of the GP index and the frequency of TC genesis very well. Clearly, determining the contributions of A, B, C, D to the term lg(*GP*) in Eq. (2) is more straightforward than evaluating the relative importance of the four variables to the GP index in Eq. (1).

The semimonthly averaged time series of each term in Eq. (2) are compared with the number of TC events in Fig.3. Terms C and D show an obvious bimodal distribution of seasonal variations. The correlation coefficients of these two terms with the number of TC events are 0.50 and 0.46, respectively, and both exceed a 95% significant level. Potential intensity in term C has the largest contribution to the increase of lg(*GP*) during late spring and autumn, whereas vertical wind shear in term D plays a relatively unimportant role as shown in Fig.3.

The BoB is a region under the significant influence of monsoon and a key location for the Asian-Pacific summer monsoon (Lin and Wang, 2002). During the monsoon onset and withdrawal over the BoB, atmospheric changes occur. Among them, the most significant change is a wind direction shift in the low atmospheric level, which is controlled by the thermal contrast between land and ocean. The dominant wind over the BoB undergoes twice changes from northeast (southwest) to southwest (northeast) at 850 hPa (200 hPa) around early May and changes back in late October (Fig.4). Thus, the vertical wind shear between 850 hPa and 200 hPa is minimum during the monsoon onset and withdrawal, and maximum in the summer and winter monsoon seasons. In addition, the vertical wind shear in summer is much larger than that in

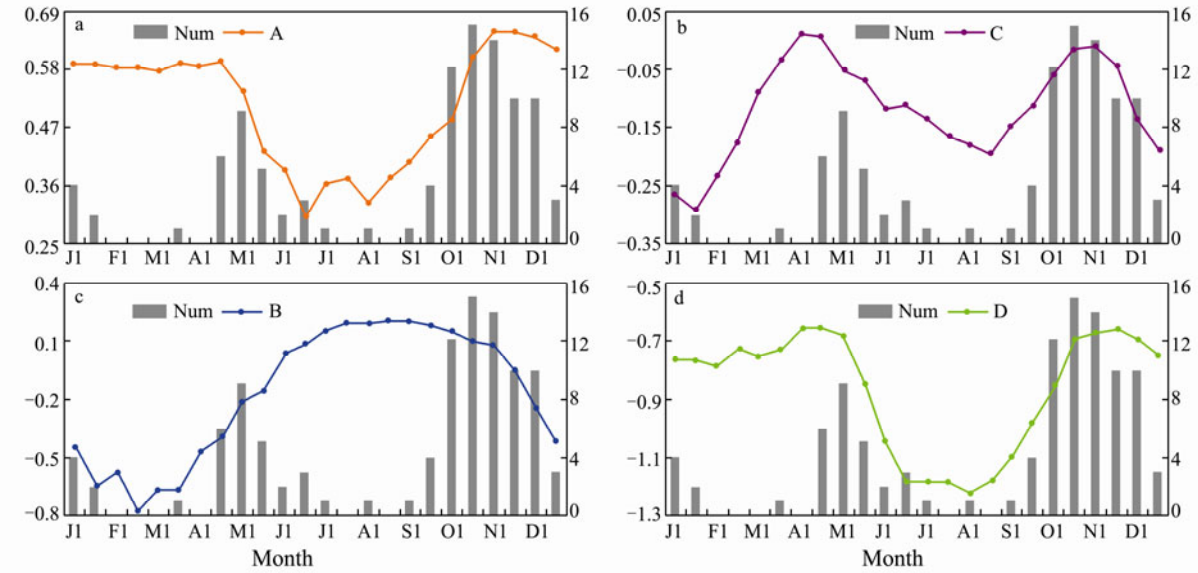

Fig.3 Seasonal variations of semimonthly averages of each variable in Eq. (2) (line) and number of TCs genesis over the BoB region (gray bar). A, B, C, and D represent the four terms on the right side of Eq. (2) respectively.

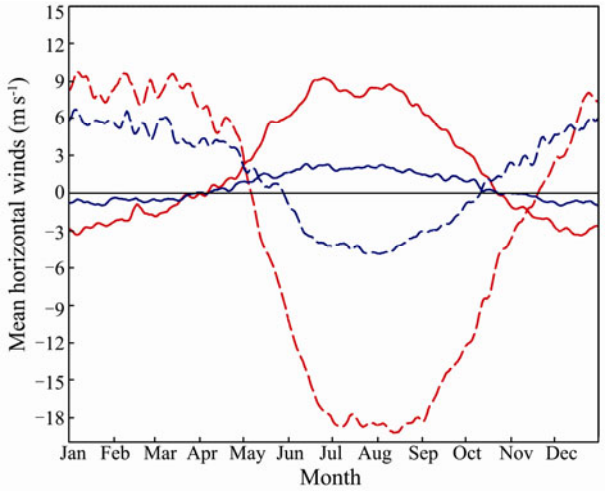

Fig.4 Annual cycle of 3-day running mean horizontal winds at 850 hPa (solid line, unit: m s^{-1}) and 200 hPa (dashed line, unit: m s^{-1}). Red represents the zonal wind and blue the meridional wind.

winter, which corresponds to the baroclinic structure related to the heat source over the Tibetan Plateau during boreal summer.

Potential intensity, greatly affected by SST, has the largest contribution to the semi-annual cycle of the TC events. Fig.5 shows the monthly climatological potential intensity (shaded) and SST (contour) over the Indian Ocean. The spatial distributions of the two variables indicate that potential intensity is well correlated with SST, which is in agreement with an empirical linear relationship between SST and potential intensity of TCs over the BoB developed by Kotal *et al*. (2009). The potential intensity associated with SST increases during April–May and October–November, and decreases in boreal summer, which is correlated with different wind speed between two transition phases and the period of the southwesterly monsoon. Corresponding to the smaller surface wind speed, the surface heat fluxes, including the latent and sensible heat fluxes, will decrease in the two periods when TC frequency peaks occur. Strong southwesterlies blowing at low-level over the BoB in boreal summer result in large amount of heat loss at the sea surface and lower SST later in boreal summer. But the low SST in boreal winter is because of the lack of solar radiation.

Generally, the bimodal distribution of TC genesis events is due to potential intensity and vertical wind shear. The fundamental reason is the change of wind direction associated with the onset and withdrawal of the summer monsoon over the BoB. The decreases of relative humidity in winter and vorticity in summer play a minor role in the contributions to the seasonal variation because the correlation of the decreases with the TC genesis frequency is rather low.

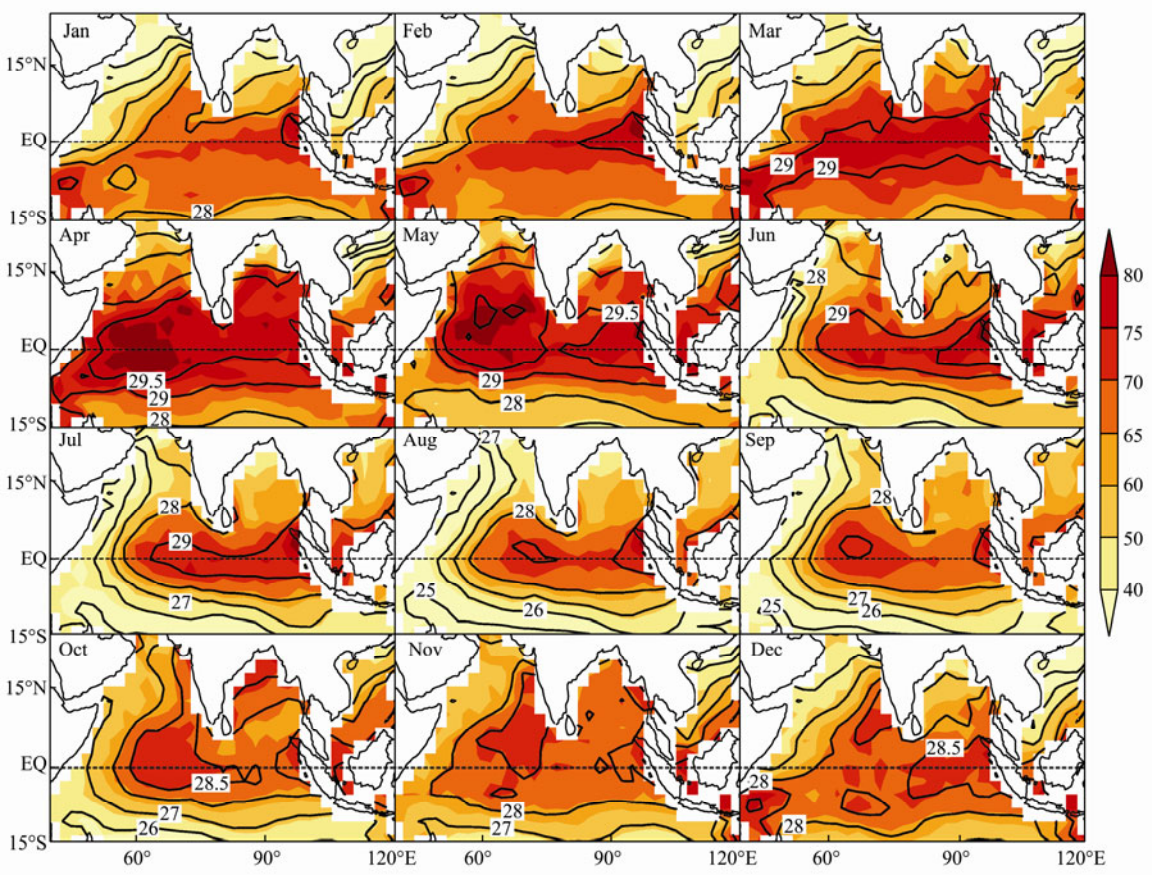

Fig.5 Comparisons of monthly climatological mean potential intensity (color, unit: m s^{-1}) and SST (contour, unit: ℃) in the Indian Ocean.

5 Monsoon Influence on Asymmetric Pattern of TC Events

5.1 Factors Affecting Monsoon Impact

Though the onset and withdrawal of the BoB summer monsoon are quasi-antisymmetric and associated with the two peaks of TC genesis, twice as many TC events occur during the second peak period compared to those during the first one. To find out what environmental conditions are responsible for this phenomenon, the differential spatial distributions of each term in Eq. (2) between early October–early November and late April–late May are examined (Fig.6).

As shown in Fig.6e, the difference of lg(*GP*) is positive over the whole basin, which is consistent with a more frequent cyclogenesis during autumn than during spring. When comparing the pattern with those shown in Fig.6a–6d, only the spatial distribution of component B illustrates the uniformity over the BoB, which shows that the relative humidity at the mid-level troposphere is the main contributor to the asymmetric pattern. Fig.6c shows that component C has negative values in most of the BoB, indicating that the potential intensity is relative high in spring than in autumn over the BoB except for the northeastern coast of the Indian subcontinent. Compared with SST in autumn (Fig.5), the higher SST in spring might be due to solar radiation as the northern hemisphere receives more during April–June and less during October–December. Thus, the potential intensity acts against the formation of the asymmetric pattern. Fig.6a (Fig.6d) also shows a change of component A (component D) from the negative (positive) in the northeast to the positive (negative) values in the southwestern part of the BoB, and the mean differences of vorticity and vertical wind shear between autumn and spring are small, which is in agreement

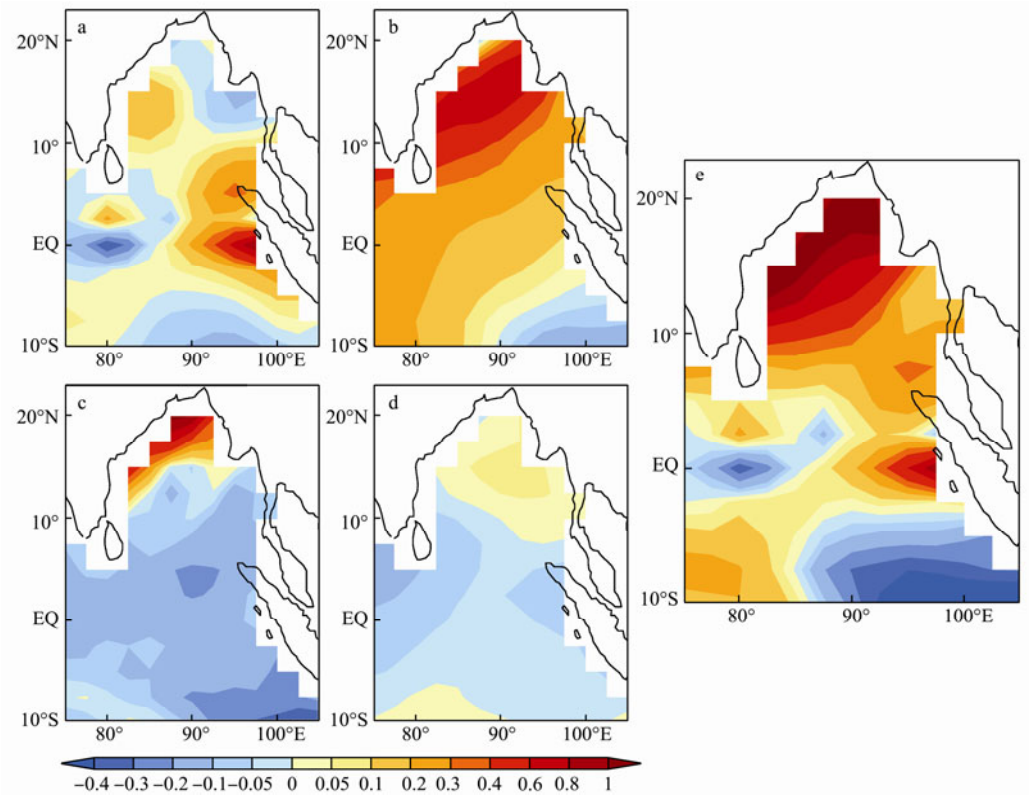

Fig.6 Spatial distributions of the differences of terms (a) A, (b) B, (c) C, (d) D, and (e) lg(*GP*) in Eq. (2) between early October–early November and late April–late May. The red (blue) color indicates that values of the terms are larger (smaller) in early October–early November than those in late April–late May.

with the results shown in Fig.3.

The ratios of area-averaged differences between each term (A, B, C, and D) and lg(*GP*) are 27.71%, 173.64%, −78.64%, and −22.71%, respectively, and the calculations demonstrate that relative humidity is the major contributor to the difference in the TC genesis frequency between autumn and late spring. The effects of vorticity and vertical wind shear are small and approximately cancel each other out, and the potential intensity plays a reversed role.

Camargo *et al*. (2007a, 2009) and Chand and Walsh (2010) recalculated the GP index to assess the individual importance of the four variables. The same method is employed in this study and the modified GP index is calculated using the annual mean climatology for three of the variables and the unmodified seasonal values for the fourth variable. The results obtained are consistent with those described in Sections 4 and 5.

5.2 Monsoon Influence on Relative Humidity

Since the difference of relative humidity between autumn and spring is important for the formation of the bimodal distribution of TC frequency, the following mois-

ture conservation equation is employed for the analysis on relative humidity:

$$\frac{\partial q}{\partial t} = -\left(\frac{\partial uq}{\partial x} + \frac{\partial vq}{\partial y}\right) - \frac{\partial \omega q}{\partial p} + S .$$

The local time tendency of moisture ($\frac{\partial q}{\partial t}$) is influenced by the divergence of horizontal moisture flux ($\frac{\partial uq}{\partial x} + \frac{\partial vq}{\partial y}$), the divergence of vertical moisture flux ($\frac{\partial \omega q}{\partial p}$), and the source/sink of moisture (S). Fig.7 displays the area-averaged divergence of horizontal moisture flux and the meridional wind over the BoB in a pressure-time domain. The positive (negative) values (shaded) indicate a divergence (convergence) of moisture flux. During November to mid-March in the next year, the northerlies dominate at the low level over the BoB, and switch to the southerlies in late March owing to the summer monsoon onset, and a similar change occurs at the middle troposphere about three months later. At 750 hPa–650 hPa, the northerlies are persistent over the BoB during February–early June, and bring in cold and dry air, which results in the divergence of horizontal moisture flux and the decrease of relative humidity for the period till mid-June. From mid-June to October appears an opposite process. The convergence of horizontal moisture flux and the increase of the relative humidity occur due to the warm wet southerlies from the tropical Indian Ocean during this period. The difference of the convergence of vertical moisture flux between late spring and autumn is small and neglected in the analysis. Therefore, the change of wind direction associated with the monsoon at the mid-troposphere is the most important contributor to the relative humidity difference between late spring and autumn, and eventually establishes the asymmetric pattern.

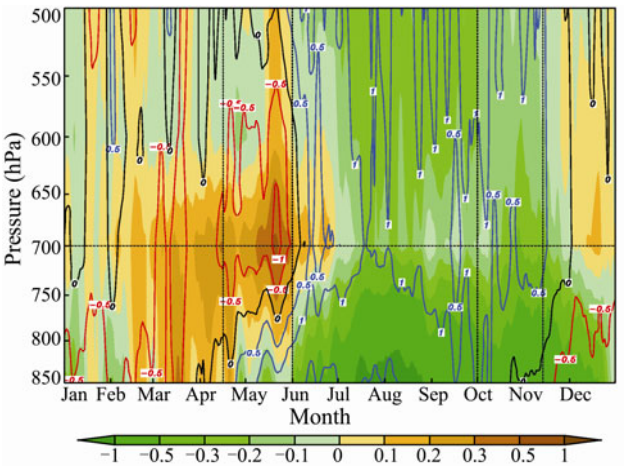

Fig.7 Area-averaged convergence of horizontal moisture flux (color) and meridional wind over the BoB (solid line, unit: m s^{-1}) in a pressure time domain. Green (dark yellow) color represents convergence (divergence) of horizontal moisture flux (unit: s^{-1}). Blue (red) line indicates a southerly (northerly) wind.

6 Conclusions

In this study the GP index is used to examine the modulation of the summer monsoon to the TC genesis frequency over the BoB. The ability of the GP index to reproduce the observed variations in TC activities is evaluated. A modified equation is also used to determine which individual physical factor comprised in the GP index is most important in causing the asymmetric bimodal distribution of TC events.

The following are the main conclusions from this study:

1) The seasonal variation of cyclogenesis over the BoB shows an asymmetric bimodal pattern. The maximum number of the TC genesis is in late October and the second largest is in early May. The two periods correspond to the withdrawal and onset of the BoB summer monsoon, respectively, which indicates the important impact of the summer monsoon on the TC genesis. The GP index tracks the monsoon-induced semi-annual climatological cycle of the TC genesis over the BoB successfully, *i.e.*, the clear suppression of the genesis during the summer and winter monsoon seasons.

2) The two peaks of TC genesis events are mainly owing to the seasonal variations of potential intensity and vertical wind shear. Because the wind speed is minimal at lower levels and 200 hPa during the periods of the summer monsoon onset and withdrawal, the vertical wind shear is rather weak and the potential intensity associated with SST reaches the maximum. The decreases of relative humidity in winter and vorticity in summer also play a role in the two suppression seasons, although relatively insignificant.

3) Relative humidity at the mid-troposphere is the major contributor to the asymmetric distribution of the TC genesis frequency between autumn and late spring. Since the change in the wind direction at 700 hPa is approximately three months later than at lower levels, the divergence of horizontal moisture flux associated with the northerlies dominates over the BoB in February-early June, and results in a lower relative humidity in late spring. The period from mid-June to October experiences an opposite process. Hence the relative humidity in autumn is much larger than that in late spring, leading to the difference of the TC genesis between the two peaks. While the potential intensity plays an opposite role in the TC genesis due to solar heating, the relative humidity shows the strongest contribution. Compared with potential intensity and relative humidity, the effects of vorticity and vertical wind shear are negligible.

Acknowledgements

We would like to thank Prof. Bin Wang of University of Hawaii for his constructive suggestions. The work was supported by the National Basic Research Program of China (973 Program: 2012CB955604), National Natural Science Foundation of China (No. 409 75038, 40830106) and the CMA Program (GYHY200906008).

References

Ahmed, R., and Karmakar, S., 1993. Arrival and withdrawal dates of the summer monsoon in Bangladesh. *International Journal of Climatology*, **13** (7): 727-740.

Ali, A., 1996. Vulnerability of Bangladesh to climate change and sea level rise through tropical cyclones and storm surges. *Water, Air and Soil Pollution*, **92** (1-2): 171-179.

Bister, M., and Emanuel, K. A., 1998. Dissipative heating and hurricane intensity. *Meteorology and Atmospheric Physics*, **65** (3-4): 233-240.

Bister, M., and Emanuel, K. A., 2002a. Low frequency variability of tropical cyclone potential intensity 1. Interannual to interdecadal variability. *Journal of Geophysical Research*, **107** (D24): 4801, DOI: 10.1029/2001JD000776.

Bister, M., and Emanuel, K. A., 2002b. Low frequency variability of tropical cyclone potential intensity 2. Climatology for 1982–1995. *Journal of Geophysical Research*, **107** (D22): 4621, DOI: 10.1029/2001JD000780.

Camargo, S. J., Emanuel, K. A., and Sobel, A. H., 2007a. Use of a genesis potential index to diagnose ENSO effects on tropical cyclone genesis. *Journal of Climate*, **20** (19): 4819-4834.

Camargo, S. J., Sobel, A. H., Barnston, A. G., and Emanuel, K. A., 2007b. Tropical cyclone genesis potential index in climate models. *Tellus A*, **59** (4): 428-443.

Camargo, S. J., Sobel, A. H., Barnston, A. G., and Klotzbach, P. J., 2010. The influence of natural climate variability on tropical cyclones, and seasonal forecasts on tropical cyclone activity. *Global Perspectives on Tropical Cyclones: From Science to Mitigation*. Chan, J. C. L., and Kepert, J. D., eds., World Scientific Series on Asia-Pacific Weather and Climate, Vol. 4, World Scientific Publishing, 325-360.

Camargo, S. J., Wheeler, M. C., and Sobel, A. H., 2009. Diagnosis of the MJO modulation of tropical cyclogenesis using an empirical index. *Journal of the Atmospheric Sciences*, **66** (10): 3061-3074.

Chand, S. S., and Walsh, K. J. E., 2010. The influence of the Madden-Julian oscillation on tropical cyclone activity in the Fiji region. *Journal of Climate*, **23** (4): 868-886.

Chu, J. H., Sampson, C. R., Levin, A. S., and Fukada, E., 2002. The Joint Typhoon Warning Center tropical cyclone best tracks, 1945–2000. *U. S. Naval Research Laboratory Rep.* NRL/MR/7540-02016, 22pp.

Emanuel, K. A., 1995. Sensitivity of tropical cyclones to surface exchange coefficients and a revised steady-state model incorporating eye dynamics. *Journal of the Atmospheric Sciences*, **52** (22): 3969-3976.

Emanuel, K. A., 2001. The contribution of tropical cyclones to the oceans' meridional heat transport. *Journal of Geophysical Research*, **106** (D14): 14771-14782.

Emanuel, K. A., and Nolan, D. S., 2004. Tropical cyclone activity and global climate. Preprints, *26th Conference on Hurricane and Tropical Meteorology*. Amer. Meteor. Soc., Miami, FL, 240-241.

Emanuel, K. A., 2005. Increasing destructiveness of tropical cyclones over the past 30 years. *Nature*, **436** (4): 686-688.

Evan, A. T., and Camargo, S. J., 2011. A climatology of Arabian Sea cyclonic storms. *Journal of Climate*, **24** (1): 140-158.

Gray, W. M., 1968. Global view of the origin of tropical disturbances and storms. *Monthly Weather Review*, **96** (10): 669-700.

Gray, W. M., 1975. Tropical cyclone genesis. *Atmospheric Science Paper*, Department of Atmospheric Science, Colorado State University, Ft. Collins, 121pp.

Gray, W. M., 1979. Hurricanes: Their formation, structure and likely role in the tropical circulation. *Meteorology over the Tropical Oceans*. Shaw, D. B., ed., Roy. Meteor. Soc., 155-199.

Hoarau, K., Bernard, J., and Chalonge, L., 2011. Intense tropical cyclone activities in the northern Indian Ocean. *Journal of Climatology*, **32** (13): 1935-1945.

Kikuchi, K., and Wang, B., 2010. Formation of tropical cyclones in the North Indian Ocean associate with two types of tropical intraseasonal oscillation modes. *Journal of Meteorological Society of Japan*, **88** (3): 475-496.

Kotal, S. D., Kundu, P. K., and Roy Bhowmik, S. K., 2009. An analysis of sea surface temperature and maximum potential intensity of tropical cyclones over the Bay of Bengal between 1981 and 2000. *Meteorological Applications*, **16** (2): 169-177.

Krishna K. M., 2009. Intensifying tropical cyclones over the North Indian Ocean during summer monsoon–global warming. *Global and Planetary Change*, **65** (1-2): 12-16.

Lander, M. A., and Guard, C. P., 1998. A look at global tropical cyclone activity during 1995: Contrasting high Atlantic activity with low activity in other basins. *Monthly Weather Review*, **126** (5): 1163-1173.

Lin, H., and Wang, B., 2002. The time-space structure of Asian summer monsoon–A fast annual cycle view. *Journal of Climate*, **15** (15): 2001-2019.

Mao, J., and Wu, G., 2006. Interannual variability in the onset of the summer monsoon over the Eastern Bay of Bengal. *Theoretical and Applied Climatology*, **89** (3-4): 155-170.

Mc Bride, J. L., 1995. Tropical cyclone formation. *Global Perspectives on Tropical Cyclones*, **693** (2): 63-105.

Pielke Jr, R. A., Rubiera, J., Landsea, C. W., Fernandez, M. L., and Klein, R., 2003. Hurricane vulnerability in Latin America and the Caribbean: Normalized damage and loss potentials. *Natural Hazards Review*, **4** (3): 101-114.

Royer, J. F., Chauvin, F., Timbal, B., Araspin, P., and Grimal, D., 1998. A GCM study of the impact of greenhouse gas increase on the frequency of occurrence of tropical cyclone. *Climatic Change*, **38** (3): 307-343.

Singh, O. P., Ali Kahn, T. M., and Rahman, M. S., 2001. Has the frequency of intense tropical cyclones increased in the North Indian Ocean? *Current Science*, **80** (4): 575-580.

Subbaramayya, I., and Rao, S. R. M., 1984. Frequency of Bay of Bengal cyclones in the post-monsoon seasnon. *Monthly Weather Review*, **112** (8): 1640-1642.

Wang, B., and Lin, H., 2002. Rainy season of the Asian-Pacific summer monsoon. *Journal of Climate*, **15** (4): 386-398.

Wu, G., and Zhang, Y., 1998. Tibetan Plateau forcing and the monsoon onset over South Asia and the South China Sea. *Monthly Weather Review*, **126** (4): 913-927.

Yanase, W., Sato, M., Taniguchi, H., and Fujinami, H., 2012. Seasonal and intra-seasonal modulation of tropical cyclogenesis environment over the Bay of Bengal during the extended summer. *Journal of Climate*, **25** (8): 2914-2930.

Yanase, W., Taniguchi, H., and Satoh, M., 2010. The genesis of tropical cyclone Nargis (2008): Environmental modulation and numerical predictability. *Journal of Meteorological Society of Japan*, **88** (3): 497-519.

(Edited by Xie Jun)